

Numerical Simulation of Fluid Structure Interaction (FSI) on a double wedge Airfoil based on Arbitrary Lagrangian-Eulerian Frameworks

Bhuiyan Shameem Mahmood Ebna Hai^{a,*} and Markus Bause^a

^a Department of Mechanical Engineering, Helmut Schmidt University,
University of the Federal Armed Forces Hamburg,
Hostenhofweg 85, 22043 Hamburg, Germany.

*shameem.ebna.hai@hsu-hh.de

Abstract. *Nowadays, advanced composite materials have shown remarkable resilience for lightweight structures, construction in ballistics protection, engineering, and other similar applications. Carbon Fiber Reinforced Plastics (CFRP) are being applied to many aircraft structures in order to improve performance and reduce the weight. But there is a possibility of structural damages due to Fluid-Structure Interaction (FSI) oscillations. Simulation of the FSI, where the dynamics of these currents dominate, poses a formidable challenge for even the most advanced numerical techniques and it is currently at the forefront of an ongoing work in Computational Fluid Dynamics (CFD). Since analytical solutions are only available in special cases, the equation needs to be solved by numerical methods. This paper focuses on the analysis of a non-linear fluid-structure interaction problem and its solution through the Finite Element Method (FEM). Here we briefly describe the analysis of incompressible Navier-Stokes and Elastodynamic equations in the arbitrary Lagrangian-Eulerian (ALE) frameworks in order to numerically simulate the FSI effect on an aircraft wing, which shall describe the underlying physics such as structural vibration. The principal aim of this research is to explore and understand the behaviour of the fluid-structure interaction during the impact of a deformable material (e.g. an aircraft wing) on air. This coupled problem is defined in a monolithic framework and different types time stepping schemes are implemented. Spatial discretization is based on a Galerkin finite element scheme. The non-linear system is solved by a Newton-like method. The implementation using the software library package DOpElib and deal.II serves best for the computation of different FSI configurations.*

Keywords: CFRP, Navier-Stokes, Elastodynamic, Lift, Drag, FSI, ALE, Vibration, FEM, DOpE lib, deal.II.

1 INTRODUCTION

This paper is intended to provide the motivation that will act as driving force for the execution of this research work. With the scope and objectives together, we will give the outline of this research to help the reader understand the context of the present proposal.

1.1 Motivation

Currently, composite materials have shown remarkable resilience for lightweight structures, construction in ballistics protection, engineering, and other similar applications. Composite materials are formed by combining two or more materials in such a way that the constituents are still distinguishable and not fully blended. The objective is usually to make a component which is strong and stiff, often with a low density. But there is a possibility of structural damage due to Fluid Structure Interaction (FSI). FSI is the interaction of some movable or deformable structure with an internal or surrounding fluid flow, which describes the coupled dynamics of fluid mechanics and structure mechanics. These types of problems are known as Classical Multi-Physics problems. The problems can be stable or oscillatory. Simulation of the FSI, where the dynamics of these currents dominate, poses a formidable challenge for even the most advanced numerical techniques and it is currently at the forefront of an ongoing work in Computational Fluid Dynamics (CFD). In this research work, we will focus on the analysis of the incompressible

Navier-Stokes and elastodynamic equations in the arbitrary Lagrangian-Eulerian (ALE) framework and present a numerical simulation of the FSI effect on an aircraft wing, in which these equations shall describe the underlying physics. For the implementation, we chose `deal.II` [2] based software package `DOPÉ lib` [3]. While widely used commercial codes, e.g. NASTRAN, FLUENT, ANSYS or COMSOL Multiphysics, can only solve particular problems of aeroelasticity and hydroelasticity and are mainly limited to linearized models, `DOPÉ lib` is a flexible toolbox providing modularized high-level algorithms that can be used to solve stationary and non-stationary PDE problems as well as optimal control problems constrained by PDEs as well as optimal control problems constrained by PDEs and Dual-Weighted-Residual approach for goal-oriented error estimation. However, FSI problems introduce new complications and complexities to be considered, such as coupling techniques, dynamic interaction, different length and time scales of subsystems, therefore making these problems much more difficult than the separate computation of the fluid and structure. But there is not enough reference papers for study the FSI effect on an aircraft wing. With this in mind, and due to the challenge that it represents, the objective of this work is to contribute to the expansion of knowledge of this specific area.

2 MATHEMATICAL MODELS

2.1 The Fluid-Structure Interaction (FSI) problem

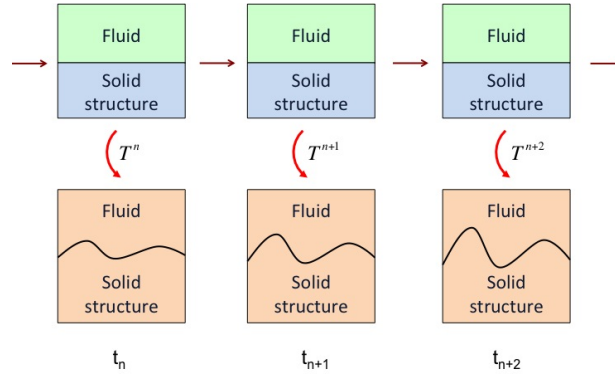


Figure 1: Typical FSI Problem in the ALE framework [7, 8, 9, 10]

Let us assume that $\widehat{\Omega} \subset \mathbb{R}^d$, $d = 2, 3$, be a bounded domain of the fluid-structure interaction problem in reference configuration at time $t = 0$ with the Lipschitzian boundary [13]. The outer unit normal vector at the boundary is denoted by n . Assume that $\Omega := \Omega(t)$ is split into two time-dependent subdomains $\Omega_f(t)$ (for an incompressible fluid flow) and $\Omega_s(t)$ (for an elastic structure), which is slicked to at the boundary of the domain $\widehat{u}_s = 0$. Here, the boundaries of Ω , Ω_f and Ω_s are denoted by $\partial\Omega$, $\partial\Omega_f$ and $\partial\Omega_s$, respectively. The variational ALE formulation of the fluid part is transformed from its Eulerian description into an arbitrary Lagrangian framework [8, 9, 10] and stated on the (arbitrary) reference domain $\widehat{\Omega}_f$, while the structure part is formulated in Lagrangian coordinates on the domain $\widehat{\Omega}_s$, where $\widehat{\Omega} = \widehat{\Omega}_f \cup \widehat{\Gamma}_i \cup \widehat{\Omega}_s$. Moreover, here we solve the Laplace equation for the definition of the ALE mapping. Here, the continuity of velocity $\widehat{v}_f = \widehat{v}_s$ and $\widehat{u}_f = \widehat{u}_s$ across the common fluid-structure interface on $\widehat{\Gamma}_i = \widehat{\Omega}_f \cup \widehat{\Omega}_s$. We search for $\widehat{u} \in H^1(\widehat{\Omega}_f, \widehat{\Gamma}_D)^d$ and $\widehat{v} \in H^1(\widehat{\Omega}_f, \widehat{\Gamma}_D)^d$, where the local quantities are defined by restrictions: $\widehat{v}_f := \widehat{v}|_{\widehat{\Omega}_f}$, $\widehat{v}_s := \widehat{v}|_{\widehat{\Omega}_s}$ and $\widehat{u}_s := \widehat{u}|_{\widehat{\Omega}_s}$. It is noted that this extension of the pressure is an inconsistency. While the fluid's pressure is of low regularity $\widehat{p}_f \in L^2_0(\widehat{\Omega}_f)$, the Laplace equation yields $\widehat{p}_s \in H^1(\widehat{\Omega}_s)$. This additional regularity will be fed back into the fluid domain if the extension is not properly decoupled. Since the ALE mapping is defined in accordance to the Lagrange-Euler structure mapping via $\widehat{T} := \widehat{x} + \widehat{u}_f$, we can define the following on all Ω : $\widehat{T} := \widehat{x} + \widehat{u}$, $\widehat{F} := I + \widehat{\nabla}\widehat{u}$, and $\widehat{J} := \det(\widehat{F})$. In the structure domain, \widehat{T} takes the place of the Lagrangian-Eulerian coordinate transformation, while in the fluid domain, \widehat{T} has no physical meaning but serves as ALE mapping.

Let us consider for a given set X , the Lebesgue space $L_X := L^2(X)$ and $L^0_X := L^2(X)/\mathbb{R}$. The functions in L_X with first-order distributional derivatives in L_X make up the Sobolev space $H^1(X)$. Furthermore, we can use

the function spaces $V_X := H^1(X)^d$, $V_X^0 := H_0^1(X)^d$, and for time-dependent functions:

$$\begin{aligned}\mathcal{L}_X &:= L^2[0, T; L_X], & \mathcal{V}_X &:= L^2[0, T; V_X] \cap H^1[0, T; V_X^*], \\ \mathcal{L}_X^0 &:= L^2[0, T; L_X^0], & \mathcal{V}_X^0 &:= L^2[0, T; V_X^0] \cap H^1[0, T; V_X^*],\end{aligned}$$

The fluid-structure interaction problem in ALE framework

Find $\hat{v} \in \hat{v}^D + \hat{\mathcal{V}}_\Omega^0$, $\hat{u} \in \hat{u}^D + \hat{\mathcal{V}}_\Omega^0$ and $\hat{p} \in \hat{\mathcal{L}}_\Omega$, such that $\hat{u}(0) = \hat{u}^0$ and $\hat{v}(0) = \hat{v}^0$, for almost all time steps $t \in I$ holds:

$$\begin{aligned}& \left(\hat{J}_f \hat{\rho}_f \partial_t \hat{v}_f, \hat{\phi}^v \right)_{\hat{\Omega}_f} + \left(\hat{J}_f \hat{\rho}_f (\hat{F}_f^{-1} (\hat{v}_f - \partial_t \hat{T}_f) \cdot \hat{\nabla}) \hat{v}_f, \hat{\phi}^v \right)_{\hat{\Omega}_f} \\ & + \left(\hat{J} \hat{\sigma}_f \hat{F}^{-T}, \hat{\nabla} \hat{\phi}^v \right)_{\hat{\Omega}_f} - \langle \hat{h}, \hat{\phi}^v \rangle_{\hat{\Gamma}_N} - \left(\hat{J} \hat{\rho}_f \hat{f}_f, \hat{\phi}^v \right)_{\hat{\Omega}_f} \\ & + \left(\hat{\rho}_s \partial_t \hat{v}, \hat{\phi}^v \right)_{\hat{\Omega}_s} - \left(\hat{\rho}_s \hat{f}_s, \hat{\phi}^v \right)_{\hat{\Omega}_s} - \left(\hat{J} \hat{\sigma}_s \hat{F}^{-T}, \hat{\nabla} \hat{\phi}^v \right)_{\hat{\Omega}_s} = 0 \quad \forall \hat{\phi}^v \in \hat{V}_\Omega^0 \quad (1) \\ & \left(\text{div}(\hat{J} \hat{F}^{-1} \hat{v}), \hat{\phi}^p \right)_{\hat{\Omega}_f} + \left(p_s, \hat{\phi}^p \right)_{\hat{\Omega}_s} = 0 \quad \forall \hat{\phi}^p \in \hat{L}_\Omega \\ & \left(\partial_t \hat{u} - v, \hat{\phi}^u \right)_{\hat{\Omega}_s} + \left(\hat{\sigma}_g, \hat{\nabla} \hat{\phi}^u \right)_{\hat{\Omega}_f} - \langle \hat{\sigma}_g, \hat{n}^f, \hat{\phi}^u \rangle_{\hat{\Gamma}_i} = 0 \quad \forall \hat{\phi}^u \in \hat{V}_\Omega^0\end{aligned}$$

The stress tensors for the fluid and structure are implemented in $\hat{\sigma}_f$, $\hat{\sigma}_s$, and $\hat{\sigma}_g$, where the stress tensors are given by $\hat{\sigma}_f(\hat{x}) = -p_f I + \hat{\rho}_f \nu_f \left(\hat{\nabla} \hat{u}_f \hat{F}_f^{-1} + \hat{F}_f^{-T} \hat{\nabla} \hat{u}_f^T \right)$, and $\hat{\sigma}_s = \hat{J}^{-1} \hat{F} \left(2\mu_s \hat{E} + \lambda_s \text{tr}(\hat{E}) I \right) \hat{F}^T$. In this formulation, for momentum equations, integration by parts in both subdomains yields the boundary term on $\hat{\Gamma}_i$ as: $\left(\hat{n}_f \cdot (\hat{J} \hat{\sigma}_s \hat{F}^{-T}), \hat{\phi}^v \right)_{\hat{\Gamma}_i} + \left(\hat{n}_s \cdot (\hat{J} \hat{\sigma}_f \hat{F}^{-T}), \hat{\phi}^v \right)_{\hat{\Gamma}_i} = 0$. We refer to [5, 7, 8, 9, 10] for more details about the functional spaces and FSI formulation in ALE formulation.

3 NUMERICAL EXAMPLE

The aim of this research is to explore and understand the behaviour of engineering artefacts in extreme environments. To achieve the main ambition of this work, we split this research into two parts. The first part will consider to determine the effect of fluid flow over a sample airfoil (2D) and study the displacement of a control point $A(t)$ under incompressible fluid flow. The second part of this research focused on FSI effect on 3D aircraft wing to identify the list of critical design points to implementing a Damage Identification Strategy (DIS) [14], where we will design an integrated SHM system for an aircraft. But numerical simulations FSI on a sample aircraft wing (3D) still in progress.

3.1 Configuration test model

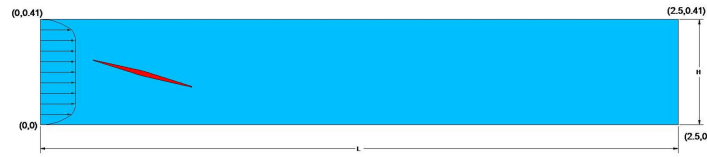


Figure 2: Computational domain

The computational domain is designed based on the 2D FSI benchmark as shown in Figure-2 and it is determined by following characteristics:

- The computational domain has the length $L = 2.5$ and height $H = 0.41$.
- We will examine a double wedge airfoil as our test model. The chord length of the airfoil $c = 0.41$ and maximum thickness $t = 0.07$ with a 15 degree angle of attack (AOA).
- Left end and right lower end of the airfoil is positioned at $(0.2, 0.253)$ and $(0.6, 0.147)$, respectively.
- The control points $A(t)$ are fixed at the trailing edge of the structure with $A(t)|_{t=0} = (0.6, 0.147)$, measuring x and y - deflections of the airfoil.

3.2 Material properties

This work is concerned with numerical approximation of FSI effect on a St. Venant-Kirchhoff (STVK) compressible elastic material model. This model is suitable for large displacements with moderate strains.

The elasticity of material structures is characterized by the Poisson ratio ν_s and the Young modulus E_{Y_s} . The relationship of two material parameters μ_s and λ_s is given by:

$$\begin{aligned}\nu_s &= \frac{\lambda_s}{2(\lambda_s + \mu_s)}, & E_{Y_s} &= \mu_s \frac{3\lambda_s + 2\mu_s}{\lambda_s + \mu_s}, \\ \mu_s &= \frac{E_{Y_s}}{2(1 + \nu_s)}, & \lambda_s &= \frac{\nu_s E_{Y_s}}{(1 + \nu_s)(1 - 2\nu_s)},\end{aligned}$$

where for compressible material $\nu_s < \frac{1}{2}$ and incompressible material $\nu_s = \frac{1}{2}$. And the fluid is assumed to be incompressible and Newtonian.

3.3 Boundary Conditions

The boundary conditions are as follows:

- A constant parabolic inflow profile is prescribed at the left inlet as

$$v_f(0, y) = 1.5U_m \frac{4y(H - y)}{H^2}, \quad (2)$$

where U_m is the mean inflow velocity and the maximum inflow velocity in $1.5U_m$

- At outlet, zero-stress $\sigma \cdot n = 0$ is realized by using the 'do-nothing' approach in the variational formulation.
- Along the upper and lower boundary, the usual 'no-slip' condition is used for the velocity.
- Left end of airfoil is considered rigid.

3.4 Initial Conditions

The initial conditions are as follows:

$$v_f(t; 0, y) = \begin{cases} v_f(0, y) \frac{1 - \cos(\frac{\pi}{2}t)}{2}, & t < 2.0 \\ v_f(0, y), & t \geq 2.0 \end{cases} \quad (3)$$

4 NUMERICAL RESULTS

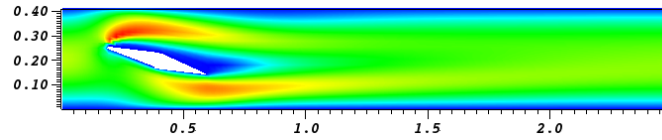
In this research, we introduce three FSI test cases that are treated with different inflow velocities (see Table-1) [8,9,10]. The parameters are chosen such that a visible transient behavior of the double wedge airfoil can be seen. To ensure a 'fair' comparison of results, we calculate the comparison values using the ALE method. For all cases, a uniform time-step size of $k = 0.0167s$ is used. But to ensure the convergence of numerical simulations, different time-step sizes and schemes are used and same result obtained.

Table 1: Parameter setting for the FSI test cases

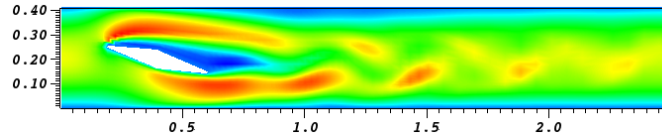
Parameter	Test-1	Test-2	Test-3
Structure model	STVK	STVK	STVK
$\rho_f [kgm^{-3}]$	1000	1000	1000
$\rho_s [kgm^{-3}]$	2710	2710	2710
$\nu_f [m^{-2}s^{-1}]$	1×10^{-3}	1×10^{-3}	1×10^{-3}
ν_s	0.33	0.33	0.33
$\mu_s [kgm^{-1}s^{-2}]$	68.9×10^6	68.9×10^6	68.9×10^6
$U_m [ms^{-1}]$	0.5	1.0	2.0

Table 2: Results for the test case 1, 2, and 3

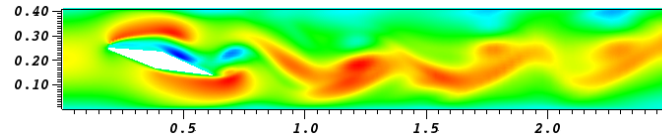
	Test-1	Test-2	Test-3
DoF	83767808	83767808	331805056
$k[s]$	0.0167	0.0167	0.0167
$u_x(A) [\times 10^{-5}]$	0.1604	0.5078 ± 0.061	2.675 ± 4.973
$u_y(A) [\times 10^{-5}]$	0.5627	1.747 ± 0.241	9.242 ± 19.219
F_D	15.693	61.025 ± 0.963	292.733 ± 84.496
F_L	24.988	69.111 ± 5.607	285.01 ± 456.08
$\Delta P [\times 10^3]$	0.138	0.827 ± 0.0295	6.306 ± 2.462



(a) Test-1



(b) Test-2



(c) Test-3

Figure 3: Velocity field

The computed values of the FSI test-1,2 and 3 are summarized in the Table-2 and the velocity fields are displayed in Figure-3. We begin with the FSI-1 test case. The time-dependent behavior of the deflections, Drag, Lift and pressure difference in between left end and right lower end of aerofoil became steady after 3.6s. Displacement in the x and y direction became steady at 0.1604×10^{-5} and 0.5627×10^{-5} , respectively. We monitored a steady pressure difference (144.751), as well as the lift and drage force 24.988 and 15.693, respectively.

In FSI test case 2 and 3, the time-dependent behavior of the displacement, pressure difference, lift and drag force are not steady. We monitored an oscillation with a range of amplitude. In a simple sense we can say that vibration is an oscillatory motion of a mechanical dynamic system or structure around same reference state, which is often the state of static equilibrium. In fact vibrations often are undesirable in mechanical structures as they cause fatigue failure and lead to increase of stress and bearing loads etc. For example, if an aircraft wing vibrates excessively, especially with the frequencies in the range of the natural frequencies (approx. 4 – 8 Hz) of the human body and organs, passengers inside the aircraft will feel uncomfortable and it can cause serious internal trauma (Leatherwood and Dempsey, 1976 NASA TN D-8188). But if aircraft wings vibrate with large amplitudes for an extended period of time, there will be fatigue failure in wings, which would potentially cause the aircraft to crash with massive fatalities. The Tacoma Narrows Bridge disaster in 1940 was one of the most famous engineering disasters of all time, and it failed due to the same type of self-excited vibration behavior that occurs in aircraft wings.

5 CONCLUSIONS

This project is focused on computing prototype configurations to test the code, which will help us to use the software to computing any realistic applications. The numerical simulations FSI on a sample aircraft wing (3D) still under test. This paper mainly deal with a double wedge airfoil (2D), where the left end of this airfoil is considered rigid and the control points $A(t)$ are fixed at the trailing edge with $A(t)|_{t=0} = (0.6, 0.147)$. We observed different behaviors of the double wedge airfoil with different FSI test cases. In test cases FSI-1, the deflection of trailing edge of the airfoil became steady, while in FSI test-2 and 3, we observed oscillating behavior. Therefore, we conclude that the deflective behavior of structures becomes unsteady under high-speed fluid flow, which can be cause of massive fatalities.

ACKNOWLEDGMENT

Thanks go to W. Wollner, T. Wick and C. Goll for developing the wonderful software packages `DOpE lib`.

REFERENCES

- [1] J. Struckmeier, “*Advanced Fluid Dynamics*”, University of Hamburg, 2011.
- [2] W. Bangerth, T. Heister, G. Kanschat, *deal.II: Differential Equations Analysis Library*, web: www.dealii.org.
- [3] C. Goll, T. Wick, W. Wollner, *DOpElib: The deal.II based optimization library*, web: www.dopelib.uni-hamburg.de.
- [4] T. Richter, “*A Fully Eulerian Formulation for Fluid-Structure-Interaction Problems*”, Institute for Applied Mathematics, University of Heidelberg, Germany, 2012.
- [5] T. Wick, “*Adaptive Finite Elements for Monolithic Fluid-Structure Interaction on a Prolongated Domain: Applied to an Heart Valve Simulation*”, Computer Methods in Mechanics, Warsaw, Poland, 2011.
- [6] T. Dunne, “*Adaptive Finite Element Approximation of Fluid-Structure Interaction Based on Eulerian and Arbitrary Lagrangian-Eulerian Variational Formulations*”, Institute for Applied Mathematics, University of Heidelberg, Germany, 2007.
- [7] T. Dunne, “*Adaptive Finite Element Simulation of Fluid Structure Interaction Based on Monolithic Variational Formulations*”, Institute for Applied Mathematics, University of Heidelberg, Germany, 2009.
- [8] H. J. Bungartz, M. Schaefer (Eds.). “*Fluid-Structure Interaction*”. Vol. 53. Springer, 2006.
- [9] Bungartz, H. J., Miriam M., Schaefer, M. (Eds.). “*Fluid-Structure Interaction-II*”. Vol. 73, 1st Ed. Springer, 2010.
- [10] G. P. Galdi, R. Rannacher, R. (Eds.). “*Fundamental Trends in Fluid-Structure Interaction*”. Vol. 1. World Scientific Publishing Co. Pte. Ltd. 2010.
- [11] W. Wollner, “*Optimization of Complex System*”, University of Hamburg, 2010-2011.
- [12] M. Hinze, “*Numerical Methods for PDEs Finite Elements*”, Department of Mathematics, University of Hamburg, 2011.
- [13] T. Richter, “*Numerical Methods for Fluid-Structure Interaction Problems*”, Institute for Applied Mathematics, University of Heidelberg, Germany, 2010.
- [14] B.S.M. Ebna Hai, M. Bause. “*Adaptive Multigrid Methods for Fluid-Structure Interaction (FSI) Optimization in an Aircraft and design of integrated Structural Health Monitoring (SHM) Systems*”. 2nd ECCOMAS Young Investigators Conference (YIC2013), Bordeaux, France, 2013.